


Article

# Biotic and Abiotic Drivers of Sap Flux in Mature Green Ash Trees (*Fraxinus pennsylvanica*) Experiencing Varying Levels of Emerald Ash Borer (*Agrilus planipennis*) Infestation

Charles E. Flower <sup>1,2,\*</sup> , Douglas J. Lynch <sup>2,3</sup>, Kathleen S. Knight <sup>1</sup> and Miquel A. Gonzalez-Meler <sup>2</sup> 

<sup>1</sup> USDA Forest Service, Northern Research Station, 359 Main Rd., Delaware, OH 43015, USA; ksknight@fs.fed.us

<sup>2</sup> Department of Biological Sciences, University of Illinois at Chicago, 845 W. Taylor St., Chicago, IL 43015, USA; doug.lynch@licor.com (D.J.L.); mmeler@uic.edu (M.A.G.-M.)

<sup>3</sup> LI-COR Biosciences, 4421 Superior Street, Lincoln, NE 68504, USA

\* Correspondence: charlesflower@fs.fed.us; Tel.: +1-740-368-0038

Received: 16 April 2018; Accepted: 24 May 2018; Published: 28 May 2018



**Abstract:** While the relationship between abiotic drivers of sap flux are well established, the role of biotic disturbances on sap flux remain understudied. The invasion of the emerald ash borer (*Agrilus planipennis* Fairmaire, EAB) into North America in the 1990s represents a significant threat to ash trees (*Fraxinus* spp.), which are a substantial component of temperate forests. Serpentine feeding galleries excavated by EAB larvae in the cambial and phloem tissue are linked to rapid tree mortality. To assess how varying levels of EAB infestation impact the plant water status and stress levels of mature green ash (*Fraxinus pennsylvanica* Marshall) trees, we combined tree-level sap flux measurements with leaf-level gas exchange, isotopes, morphology and labile carbohydrate measurements. Results show sap flux and whole tree water use are reduced by as much as 80% as EAB damage increases. Heavily EAB impacted trees exhibited reduced leaf area and leaf mass, but maintained constant levels of specific leaf area relative to lightly EAB-impacted trees. Altered foliar gas exchange (reduced light saturated assimilation, internal CO<sub>2</sub> concentrations) paired with depleted foliar  $\delta^{13}\text{C}$  values of heavily EAB impacted trees point to chronic water stress at the canopy level, indicative of xylem damage. Reduced photosynthetic rates in trees more impacted by EAB likely contributed to the lack of nonstructural carbohydrate (soluble sugars and starch) accumulation in leaf tissue, further supporting the notion that EAB damages not only phloem, but xylem tissue as well, resulting in reduced water availability. These findings can be incorporated into modeling efforts to untangle post disturbance shifts in ecosystem hydrology.

**Keywords:** emerald ash borer (*Agrilus planipennis*); invasive species; *Fraxinus*; forest disturbance; sap flux; tree water use; thermal dissipation probe

## 1. Introduction

Patterns of sap flux in trees are used in estimates of whole-tree water use, tree-level transpiration, and are even scaled to ecosystem transpiration, as such precise measurements of water exchanges are essential for coupled biosphere-atmosphere models. The variables driving water fluxes through the soil-plant continuum are generally well understood [1–4]. However, the impacts of biotic factors such as tree boring forest pests on host water use are largely understudied (but see [5]), despite the considerable impacts they have on forest systems [6]. Abiotic variables including light levels, vapor pressure

deficit (VPD), and soil moisture have long been shown to drive sap flux, generally with higher irradiance, higher VPD, and lower soil moisture driving higher rates of sap flux [2,7,8]. From a biotic standpoint, substantial variability has been shown to occur among species [9–11], between trees of the same species which differ in size [2], and based on tree canopy position (i.e., dominant, codominant or suppressed) [12]. Several studies have demonstrated reduced sap flux and water use associated with the disease progression and susceptibility of host trees to fungal pathogens (e.g., [13–16]) as well as forest response to defoliation (e.g., [17,18]). To date, we could identify only a single study describes tree-level sap flux declines following a tree boring beetle attack (i.e., mountain pine beetle (*Dendroctonus ponderosae* Hopkins) infestation of lodgepole pine (*Pinus contorta* Douglas) [5]. When assessing the impacts of biotic forest disturbances on tree sap fluxes however, potentially unique characteristics of a given disturbance agent may result in a variety of responses necessitating further investigation.

Emerald ash borer (*Agrilus planipennis* Fairmaire, EAB) is a tree-boring beetle native to Asia, which was inadvertently imported into the United States in the 1990s [19–23]. Emerald ash borers feed almost exclusively on trees in the genus *Fraxinus* [24,25], but see [26] whose constituent species are widely distributed across xeric (e.g., *F. Americana* L., *F. quadrangulata* Michx.), mesic (e.g., *F. pennsylvanica* Marshall) and hydric (e.g., *F. nigra* Marshall, *F. profunda* Bush) forests in the continental US [27–29] and southern Canada [30]. In forests of the Great Lakes Region of the U.S., ash occupies an ecologically important niche in riparian and wetland systems and accounts for ~5–9% of aboveground live carbon mass [28]. Unlike most native tree boring beetles which typically attack trees experiencing physiological stress, in its invaded range EAB attacks healthy and stressed trees, with preference for damaged trees [31]. EAB causes progressive canopy decline [32] that culminates with ash tree mortality in 2–5 years and almost complete ash tree mortality at the forest level within 6 years [33]. It is generally recognized that EAB larvae cause rapid tree mortality via their feeding in the cambial and phloem tissue, which creates serpentine galleries that sever sap transport between shoots and roots [22,34,35]. While simulated girdling studies have been conducted to assess the decline of black ash in wetlands (*F. nigra*) [36], the effects of EAB on tree-level water uptake and sap flux remain undocumented. Thus, direct evidence of the physiological mechanisms altered by EAB infestation are lacking. Changes in water relations caused by EAB will not only accelerate the rate of tree mortality, but also may have local consequences for surface hydrology and the energy balance of associated ecosystems [6,37].

Forest pests that damage cambial tissue can impact tree water use and canopy processes by at least three non-exclusive mechanisms. First, forest pests can impact tree water use via direct feedback mechanisms that regulate photosynthesis [38]. Specifically, leaf stomatal closure may be caused by direct loss of turgor pressure in guard cells associated with changes in the hydraulic conductance along the soil-leaf continuum [39–41] or by increased concentrations of free abscisic acid [42]. Second, the sink limitation imposed by the forest pest's girdling behavior may result in the accumulation of photosynthate in source leaves [43] causing down regulation of photosynthesis, photoinhibition and related effects [44]. Third, via persistent and chronic direct mechanical damage to vascular tissue over a period of years, impacted trees may exhibit reduced leaf area at both canopy and single leaf levels, resulting in concomitant reductions in water use [45,46]. Understanding the underlying mechanisms involved in ash tree responses to EAB will facilitate a better understanding of the associated hydrological responses to forest pests [36]. Studying these effects on EAB impacted forests is of particular importance because our understanding of the hydrological responses to forest pest disturbances predominantly rely largely on girdling studies or inoculations of fungal pathogens, whose damage symptom progressions differ at the tree level. Specifically, sap flux measurements studying mortality from fungal pathogen inoculations can occur in as few as 1 year [14,15], girdling in as quickly as 2 years [47], and EAB induced mortality from 2–5 years [33].

The objective of this study was to examine the impacts of the invasive EAB on ash foliar morphology and tree water use within an ash dominated forest in central Ohio, U.S. The even-aged

forest stand utilized in this study is comprised of mature overstory green ash (*F. pennsylvanica* Marshall) trees displaying all stages of EAB infestation [35], thus providing a unique opportunity to investigate biotic (i.e., EAB) and abiotic drivers of tree water use. Using Granier type sap flux probes (described by Lu et al. [8]), we measured sap flux density as a proxy for direct water use in nine green ash which comprised the full range of EAB impacted conditions. We also measured the bulk leaf carbon (C) isotopic composition,  $\delta^{13}\text{C}_{\text{leaf}}$ , of leaf tissue from the focal trees as a proxy for relative changes in intrinsic water use efficiency (the ratio of water used per carbon gain at the leaf level) [48]. Foliar nonstructural carbohydrate concentrations were measured to assess sink limitations [43]. Finally, we conducted leaf level gas exchange measurements of canopy leaves and collected leaf tissue from the canopy of ash trees across a gradient of EAB induced mortality to assess morphological characteristics (surface area (SA), dry mass (DM), and specific leaf area (SLA)). These parameters are used to elucidate the plant hydrological consequences of EAB infestation and to assess the role of water on mortality of infected ash.

## 2. Materials and Methods

### 2.1. Site Description and Tree Selection

This study was conducted in 2010 within a 35-year old (as determined dendrochronologically) abandoned tree plantation established on an agricultural field in central Ohio located at the USDA Forest Service Northern Research Station (40° 23' N, 83° 02' W) previously described by Flower et al. [49]. Following abandonment ~30 years prior to the study, succession occurred unimpeded. The forest is characterized by silty loam soils, is at an elevation of 290 m above sea level, and its average annual precipitation from 2006–2010 was 92.04 cm  $\pm$  3.71 cm. The forest canopy is dominated by *F. pennsylvanica* (green ash) and *F. americana* L. (white ash), which represent ~80% of tree basal area, as well as *Ulmus americana* L. (American elm), and *Tilia americana* L. (basswood).

Green ash trees were selected for inclusion in the sap flux study by first assessing the diameter at breast height (DBH, ~1.37 m from ground) of each tree in the forest stand and if an ash tree, rating the ash canopy condition (see below for description of AC classes). Additionally, the height of each tree was measured prior to the study with a hypsometer (Vertex IV; Hagl f, Sweden). Nine trees of comparable DBH were randomly selected within the plot across the range of AC classes (see Table 1 for more details on study trees). Investigative sap flux studies have been successfully conducted with low replication when the effect sizes for the variables of interest are large [13,50]. Only co-dominant overstory ash trees were selected for sap flux measurements, since canopy position has been shown to impact sap flow rates [51]. Selected trees were located >10 m from the forest edge to minimize the microclimatic variability and differences in turbulence and momentum fluxes near forest edges which can impact canopy level boundary conditions, transpiration and sap flux rates [52–55]. Measurements of solar radiation and VPD were derived from a meteorological station located at the USDA FS station <0.5 km from the study site.

**Table 1.** Characteristics of the experimental *Fraxinus pennsylvanica* sampled for sap flux density.

Tree No.	AC	DBH <sup>a</sup> (cm)	Tree Height (m)	Avg. Daily Sap Flux (kg/day $\pm$ se)	Leaf $\delta^{13}\text{C}$	% EAB Gallery Cover
1	1	18.8	11.9	13.69 $\pm$ 0.33	−28.12	0
2	1	22.4	13.2	13.13 $\pm$ 0.10	−28.11	5
3	1	17.8	11.2	13.01 $\pm$ 0.31	−27.39	5
4	2	20.1	12.1	4.54 $\pm$ 0.30	−26.97	10
5	2	19.8	12.3	3.78 $\pm$ 0.28	−25.94	17.5
6	3	19.3	11.6	3.74 $\pm$ 0.16	−26.49	25
7	4	17.0	10.5	2.20 $\pm$ 0.15	−25.91	45
8	4	18.2	11.7	1.17 $\pm$ 0.22	−25.94	50
9	4	18.8	11.5	1.48 $\pm$ 0.10	−25.92	55

<sup>a</sup> Diameter at breast height.

Each live co-dominant ash tree within the interior of the stand was evaluated for EAB infestation using a visual assessment of canopy health called ash canopy condition (AC). This visual assessment has been shown to exhibit a significant relationship with tree-level EAB densities (larvae/adult) and EAB gallery cover and thus it represents a solid visual proxy for EAB infestation levels [35,56]. Briefly, ash canopy condition is graded on a 1 (healthy) to 5 (dead) scale: (1) healthy/full canopy—a healthy ash canopy is full and exhibits no defoliation; (2) thinning canopy—slight reduction in leaf mass, all top branches exposed to sunlight have leaves; (3) dieback—canopy is thinning and some top branches exposed to sunlight are defoliated, lower branches which exhibit natural thinning are not considered; (4) >50% dieback—the canopy has less than 50% of the leaves of a class 1 tree and/or over half of the top branches are defoliated; and (5) dead canopy—no leaves remain in the canopy portion of the tree, regardless of epicormic sprouts [57]. Canopy condition was determined visually in June after leaf expansion was complete. Additionally, EAB larval gallery cover was quantified on 22 August 2018 following termination of sap flux measurements on two debarked 10 × 10 cm windows (on the north and south side of each tree) at 1.5 m height as described by Flower et al. [35].

## 2.2. Sap flux Measurements

Granier [58] type systems consisting of thermal dissipation probes (TDP, manufactured by PlantSensors, Nakara, Australia) were deployed to measure sap flux in nine ash trees along a gradient of EAB infestation. Each system is a pair of TDP probes (each 2 mm in diameter) inserted radially into the sapwood of the bole to a depth of 2 cm and separated vertically, with the upper probe heated and the lower probe an unheated reference. Two TDP systems were deployed per tree at a height of 1.37 m, one on the north-facing side and one on the south facing-side of each tree to account for flux variability along the stem circumference. In all trees, the depth of the sapwood exceeded the depth of the TDP. The heated and reference probes were placed ~10 cm apart (so the reference measurements are not affected by the heating) and the heating power was adjusted to 0.2 W and induced a maximum temperature difference of 8–10 °C under zero flux conditions as described by Do and Rocheteau [59]. In order to reduce the effect of natural temperature gradients which can impact measurement accuracy, we utilized a heating/cooling cycle of 15 min/15 min as described by Do and Rocheteau [59]. Additionally, the TDP systems were surrounded by closed cell foam and wrapped in a reflective heat shield (a foil coated bubble sheet ~0.6 m in height, wrapped around the TDP system and tree) to minimize temperature gradients associated with direct radiation. Silicone caulking was used at the top and bottom of the heat shield to exclude rain and stem flow from interfering with the TDP systems. Sap flux probes were deployed on 17 June 2010 and data was recorded through 1 August, because of interference with the sap flux probes from raccoons we will only report results from before this interference (17–20 June). Temperature differentials were measured every 5 min between the heated and reference thermocouple junctions on each probe and 30 min means were recorded on a Campbell CR10 datalogger (Campbell Scientific, Logan, UT, USA). Temperature differentials between probes were influenced by sap flux density surrounding the heated probe. Sap flux density (SFD,  $\text{m s}^{-1}$ ) for each sensor was calculated according to Granier [12,58] using the following equations:

$$\text{SFD} = \alpha K^\beta, \quad (1)$$

where  $\beta = 1.231$  and  $\alpha = 119 \times 10^{-6} \text{ m s}^{-1}$  [59]. The flux index (K, a dimensionless value) is defined as:

$$K = (\Delta T_0 - \Delta T_u) / \Delta T_u, \quad (2)$$

where  $\Delta T_0$  is the maximum temperature difference obtained under zero flux conditions and  $\Delta T_u$  is the measured temperature difference at a given flux density. It was assumed that no sap flux occurred at pre-dawn. Tree level water use (TWU,  $\text{kg h}^{-1}$ ) was calculated as:

$$\text{TWU} = \text{SFD} \times S_A, \quad (3)$$

where  $S_A$  is the cross-sectional area of the sapwood at the level of the heating probe [12]. The cross-sectional area of sapwood was estimated visually, by wood color as described by Meadows and Hodges [60], from increment cores removed following sap flux measurements. Daily tree level water use ( $TWU_D$ ,  $\text{kg}^{-1} \text{ day}^{-1}$ ) was calculated as the 24-h daily sum of TWU. In summary, as sap flows past the unheated (lower) thermocouple, it records the ambient sap temperature and the upper heated needle is cooled. Rapid sap flux results in low differences in the thermocouple temperatures as the upper (heated) thermocouple is cooled.

### 2.3. Leaf Tissue Sampling

In late June 2010, leaf tissue was excised from the upper sun exposed canopy of each focal (sap flux) ash tree during mid-day using a shotgun. Collected leaf tissue from each experimental ash tree was immediately oven-dried at  $60^\circ\text{C}$  for  $\sim 48$  h to constant mass to remove any moisture prior to isotopic analysis. The bulk leaf carbon isotopic composition,  $\delta^{13}\text{C}$ , represents an unbiased integrator of a plant water relations over the longevity of the leaf tissue and can be used as a surrogate for intrinsic water use efficiency. The intrinsic water use efficiency is non-linearly proportional to the difference between ambient  $\text{CO}_2$  concentrations ( $C_a$ ) and internal leaf  $\text{CO}_2$  concentrations ( $C_i$ ) [48]. Thus, under constant  $C_a$ , and constant  $\delta^{13}\text{C}$  of atmospheric  $\text{CO}_2$ ,  $\delta^{13}\text{C}$  reflects a relative and integrated measure of intrinsic water use efficiency among trees of different AC.

On 11–12 July 2013, at least 3 replicate leaf samples were collected from the upper sun exposed canopy of 20 ash trees across a gradient of AC classes to assess differences in leaf morphology. Leaf tissue was collected from 09:00–10:30 and the surface area determined immediately following collection using a LI-COR 3100 leaf area meter (LI-COR, Lincoln, NE, USA). Samples were then dried in a forced-air convection oven at  $60^\circ\text{C}$  for 48 h or until no change in mass was detected and analyzed for % carbon (%C), % nitrogen (%N), and  $\delta^{13}\text{C}$  as described below. Replicates were averaged prior to statistical analyses.

### 2.4. Foliar Gas-Exchange Measurements

During June 2015, sun-exposed branches were collected between 09:30–11:30 from the upper canopy of green ash trees across the AC gradient ( $n = 12$  trees). Branches were re-cut under deionized water to reduce embolism and gas-exchange measurements were conducted immediately thereafter. An open-system portable IRGA (LI-6400 equipped with the 6400-02 LED light source attachment, LI-COR, Inc., Lincoln, NE, USA) was used to measure the light saturated photosynthetic rate ( $A_{\text{sat}}$  @ 1600 PAR;  $\mu\text{mol CO}_2 \text{ m}^{-2} \text{ s}^{-1}$ ), internal  $\text{CO}_2$  concentrations ( $C_i$ ; ppm  $\text{CO}_2$ ), and stomatal conductance (gs;  $\text{mmol m}^{-2} \text{ s}^{-1}$ ) for 3 fully expanded leaves/branch. Before each measurement the leaf chamber was checked for leaks and stability in flow ( $500 \mu\text{mol s}^{-1}$ ),  $\text{CO}_2$  (400 ppm), and  $\text{H}_2\text{O}$  (<80%).

### 2.5. Elemental and Isotopic Analysis of Leaf Tissue

Dried plant tissue was finely ground using a ball mill prior to analysis. The carbon content of leaf tissue was made via flash combustion using a Costech Elemental Analyzer (Valencia, CA, USA) with a zero-blank autosampler and electronic actuator to eliminate air contamination in the samples. Stable isotope analyses of C were conducted on the same sample using an IRMS (isotope ratio mass spectrometer, Finnigan Deltaplus XL, Bremen, Germany) operated in continuous flow mode and calibrated to the  $^{13}\text{C}$  Vienna PeeDee Belemnite (VPDB) scale using USGS 40 with a precision of 0.05‰. Elemental and solid international and secondary isotope standards were used for instrument calibration and sample conversion to  $\delta$  values. Isotopic values are reported in delta notation relative to the standard VPDB for carbon, ( $\delta_{\text{sample}} = 1000 ((R_{\text{sample}}/R_{\text{standard}}) - 1)$ ,  $R = ^{13}\text{C}/^{12}\text{C}$ ). All measurements were done at the stable isotope laboratory at the University of Illinois at Chicago.



## 2.6. Plant Tissue Non-Structural Carbohydrate Analysis

In 2010, leaf tissue (as previously described) from sap flux trees was analyzed for nonstructural carbohydrates (starch and soluble sugars; NSC). Briefly, we quantified soluble sugars and starch in woody tissues using standard methods [61]. Leaf tissue was dried in a forced convection oven immediately following collection until no mass loss and ground with a ball mill for 3 min. Soluble sugars (sucrose, glucose, and fructose) were extracted from 25 mg of tissue with 80% ethanol (5 mL) at 80 °C for 5 min. Extracts were centrifuged and the supernatants pooled; a 2 mL aliquot was removed and dried using a vacuum evaporator. Dried extract was resuspended with 3 mL deionized water and 40 mg polyvinylpyrrolidone and spun down using a centrifuge. A 0.5 mL aliquot was colorimetrically assayed for soluble sugars [61] and modified for use on deciduous tissues according to Curtis et al. [62]. Soluble sugar recovery was >95%.

Starch was quantified from the soluble sugar extracted tissue pellets by resuspension using 1 mL of 0.2 N KOH and incubated at 80 °C for 25 min. KOH was neutralized by adding 0.2 mL of 1 N acetic acid. Starch was hydrolyzed to glucose with  $\alpha$ -amylglucosidase solution (pH 7.05) at 55 °C for 1.5 h and assayed according to Jones et al. [61]. Starch recovery was >95%. The total nonstructural carbohydrate concentration (TNC) was the sum of soluble sugars and starch.

## 2.7. Statistical Analysis

The effect of AC on ash tree sap flux density rates (SFD) were investigated using a repeated measures analysis of variance (RM ANOVA) test, with the hourly SFD measurements as the repeated measure. Sap flux density rates were compared between AC using Tukey's HSD,  $\alpha = 0.05$ . Because of lack of replication, trees in AC 2 and 3 were pooled prior to analysis and thus represent a moderate level of EAB decline. Separately, we tested the role of AC and abiotic factors on SFD using ANOVA, in which AC was treated as a main effect and the environmental parameters (radiation and VPD) were treated as covariates. Additionally, the effect of AC on average  $TWU_D$  were tested using ANOVA, daily tree level water use was compared between AC using Tukey's HSD,  $\alpha = 0.05$ . The relationship between daily sap flux rates and the carbon isotopic composition of leaf tissue ( $\delta^{13}C_{Leaf}$ ) was tested using Spearman's Rank Correlation Analysis, due to the non-linear relationship between daily sap flux rates and the carbon isotopic composition of leaf tissue ( $\delta^{13}C_{Leaf}$ ). This test provides a distribution free test of independence between the variables. The effect of ash condition classes (AC) on morphological leaf measurements (surface area, dry mass, specific leaf area), gas exchange parameters ( $A_{sat}$ ,  $g_s$ , and  $C_i$ ) and leaf carbon isotopic composition were investigated using independent analysis of variance (ANOVA) tests. Variables were compared between AC classes using Tukey's HSD,  $\alpha = 0.05$ . The effect of AC on leaf starch, soluble sugar, and TNC concentrations was assessed with ANOVA, trees in AC 2 and 3 were pooled prior to analysis. All statistical analyses were conducted using SYSTAT statistical software (v13, SYSTAT 2007).

## 3. Results

### 3.1. Sap Flux Density Rates by Ash Canopy Condition Classes and Abiotic Drivers

Sap flux densities ranged from 0.00 to 1.49  $m\ s^{-1}$  and exhibited significant variability attributed to ash canopy condition classes (ANOVA;  $F_{(26,24)} = 566.3$ ,  $p < 0.001$ ). Sap flux densities in healthy trees (AC 1;  $0.583\ m^3\ m^{-2}\ s^{-1} \pm 0.045\ SE$ ) were significantly higher than those of moderately (AC 2 or 3;  $0.144\ m^3\ m^{-2}\ s^{-1} \pm 0.011\ SE$ ) and heavily (AC 4;  $0.112\ m^3\ m^{-2}\ s^{-1} \pm 0.009\ SE$ ) infested ash trees (Tukey's HSD  $p < 0.001$  for all AC values; Figure 1). Sap flux density also exhibited significant temporal variability across the sampling period (ANOVA;  $F_{(103,624)} = 105.018$ ,  $p < 0.001$ ). Finally, we observed a significant difference in the interaction term (AC  $\times$  time), highlighting increased responsiveness in sap flux in the healthy trees over time (Figure 1; ANOVA;  $F_{(206,624)} = 36.251$ ,  $p < 0.001$ ).

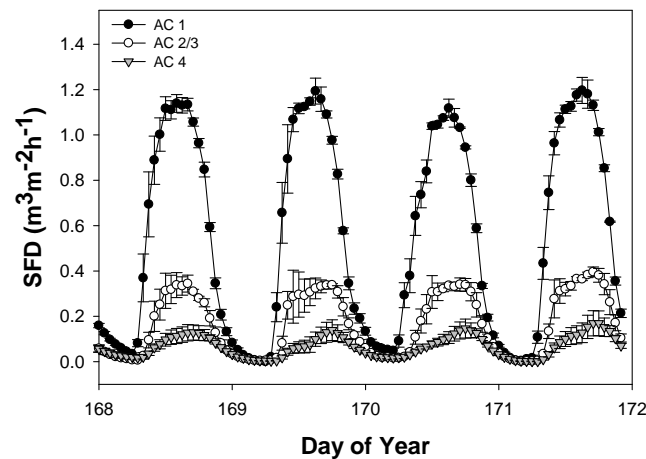


**Figure 1.** Sap flux density (SFD) of *Fraxinus pennsylvanica* trees during 26–30 June 2010 (AC1 = low infestation levels, AC 2 & 3 moderate infestation levels, and AC4 = high infestation levels). Error bars denote  $\pm 1$  SE.

Although substantial variation existed between AC classes and over time, SFD exhibited considerable diurnal fluctuations within trees generally peaking during mid-day when the evaporative demand was greatest (Figure 1; Table 2). The SFD was most strongly driven by incoming solar radiation and VPD (Table 2). Higher order interactions of AC\*VPD and AC\*radiation were also significant, indicating the differential impacts that the abiotic factors have on the SFD of trees across different AC classes (Table 2). Specifically, SFD was less responsive to increased radiation as EAB induced canopy decline manifested (Figure 2).

**Table 2.** Analysis of variance statistics for the main effects of ash canopy condition class, vapor pressure deficit (VPD), and radiation on ash tree sap flux (SFD) density rates.

Source	Type III SS	df	MS	F-Ratio	p-Value
AC	0.215	2	0.108	7.34	0.001
VPD	0.904	1	0.904	61.65	<0.001
Radiation	11.867	1	11.867	809.37	<0.001
AC $\times$ VPD	0.426	2	0.213	14.53	<0.001
AC $\times$ Radiation	7.441	2	3.721	253.76	<0.001
AC $\times$ VPD $\times$ Radiation	1.562	2	0.781	53.284	<0.001
Error	13.562	925	0.015		

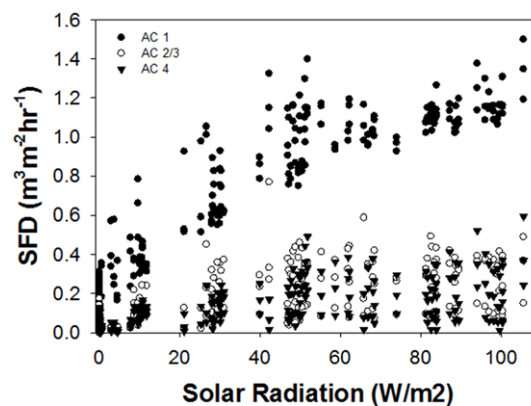


**Figure 2.** Half hourly sap flux density (SFD) of *Fraxinus* trees in relation to solar radiation ( $W/m^2$ ) during 26–30 June 2010 (AC1 = low, AC2/3 = moderate, AC 4 = high infestation levels).

### 3.2. Daily Sap Flux

Reduced tree level SFD resulted in significant differences in daily sap flux rates ( $TWU_D$ ) between lightly and heavily infested trees (Figure 3, ANOVA;  $F_{(2,6)} = 554.014$ ;  $p < 0.001$ ). Values of  $TWU_D$  tended to be greater for trees which were lightly or not infested with EAB (AC 1 =  $13.27 \text{ kg day}^{-1} \pm 0.25 \text{ SE}$ ) relative to moderately (AC 2 & 3 =  $4.02 \text{ kg day}^{-1} \pm 0.31 \text{ SE}$ ) and heavily infested trees ( $1.62 \text{ kg day}^{-1} \pm 0.37 \text{ SE}$ , Figure 3). Furthermore, a Spearman's rank correlation revealed that  $TWU_D$  was negatively correlated with the  $\delta^{13}\text{C}_{\text{Leaf}}$  ( $r_s = -0.9372$ ,  $p < 0.05$ ).

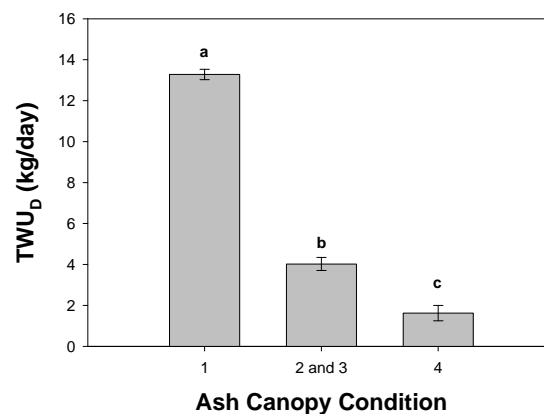


**Figure 3.** Mean daily sap flux ( $TWU_D$ ) across trees of different ash condition classes. Letters represent significance levels determined by Tukey's HSD pairwise comparisons ( $p < 0.05$ ), error bars denote  $\pm 1 \text{ SE}$ .

### 3.3. Leaf Traits

Individual leaf surface area varied from  $7.1$  to  $41.2 \text{ cm}^2$  and was significantly larger in healthy trees (AC 1 and AC 2) relative to trees exhibiting EAB induced canopy decline (AC 3 and AC 4) (Figure 4A; ANOVA;  $F_{(3,16)} = 10.731$ ,  $p < 0.001$ ). Leaf dry mass was also significantly larger in healthy trees (AC 1 and AC 2) relative to trees exhibiting canopy decline (AC 3 and AC 4) (Figure 4B; ANOVA;  $F_{(3,16)} = 9.026$ ,  $p = 0.001$ ). As such, leaf dry mass exhibited a linear positive relationship with leaf surface area (Figure S1; Adj  $r^2 = 0.98$ ). Because of the conserved relationship between leaf dry mass and leaf surface area, no significant differences were observed in the specific leaf area (data not presented;  $p = 0.472$ ).

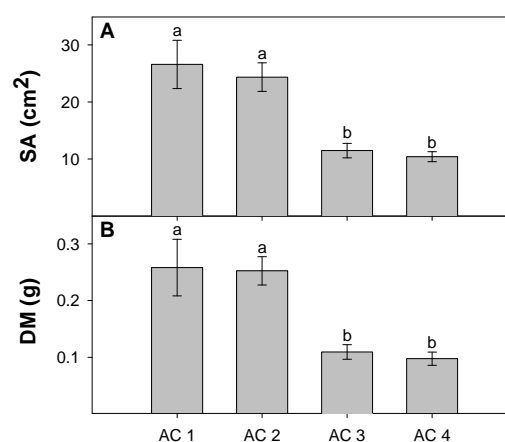


**Figure 4.** Leaf surface area (SA) (A) and leaf dry mass (DM) (B) in relation to ash tree canopy condition class (AC). Significance levels depict results of Tukeys HSD pairwise comparisons ( $p < 0.05$ ).



### 3.4. Foliar Chemistry

Leaf carbon isotopic signatures exhibited significant enrichment along with progressive canopy decline (Figure 5A; ANOVA;  $F_{(3,16)} = 9.08, p < 0.001$ ), while no significant differences were observed in the foliar nitrogen isotopic signatures (Figure 5B; ANOVA;  $F_{(3,16)} = 2.152, p = 0.134$ ). Bulk leaf carbon content generally increased as ash canopy condition increases. The carbon content of leaves in AC 1 was significantly lower than that of trees in AC 2 and AC 4 (Posthoc Tukey's HSD  $p < 0.05$ ; data not shown). Bulk leaf nitrogen content also exhibited variability across AC classes, although differences were less pronounced, and AC 1 was only different than AC 2 and AC 3 (Posthoc Tukey's HSD  $p < 0.05$ ; data not shown). High foliar bulk N and low bulk C in the foliar tissue of trees in AC 1 largely led to the significant differences in leaf C:N ratios between AC classes (Figure 5C; ANOVA;  $F_{(3,16)} = 6.241, p = 0.005$ ).

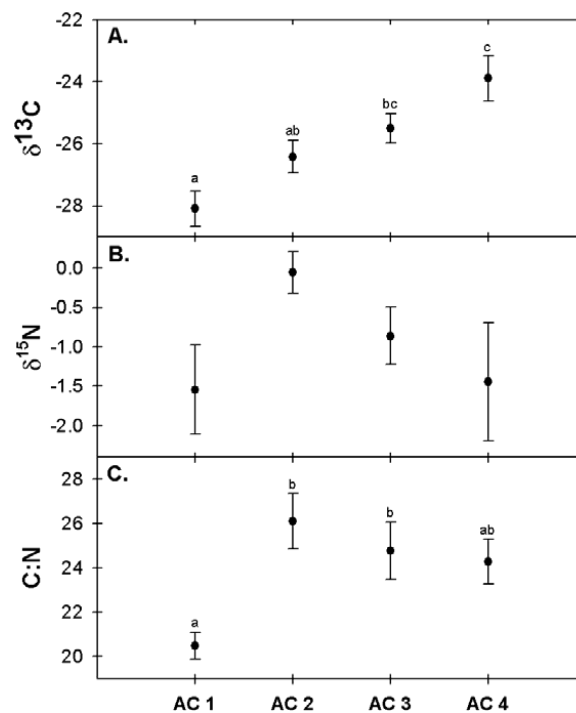


**Figure 5.** Relationship between green ash foliar  $^{13}\text{C}$  and ash canopy decline (A), foliar  $^{15}\text{N}$  (B), and foliar carbon to nitrogen ratio (C). Significance levels depict results of Tukeys HSD pairwise comparisons ( $p < 0.05$ ).

Soluble sugar concentrations ranged from 13 to 51  $\text{mg g}^{-1}$  and starch concentrations ranged from 1.2 to 22  $\text{mg g}^{-1}$  (see Table 3 for means). In general, foliar soluble sugar concentrations were greater than starch concentrations (Table 3). No significant differences in soluble sugar ( $p = 0.13$ ), starch ( $p = 0.361$ ), or TNC concentrations ( $p = 0.66$ ) were observed between AC classes.

**Table 3.** Foliar soluble sugar, starch concentrations, and total nonstructural carbohydrates (TNC) ( $\text{mg/g}$ ) between ash canopy condition classes. Values represent mean and (SE). No significant differences across AC classes were observed between soluble sugars, starch, or TNC concentrations were revealed via one-way ANOVA.

AC	Soluble Sugars	Starch	TNC
1	38.0 (0.9)	4.9 (1.5)	42.9 (2.3)
2/3	46.1 (4.0)	4.7 (2.3)	50.8 (2.1)
4	28.3 (7.9)	12.0 (5.9)	40.3 (13.8)

### 3.5. Foliar Gas Exchange

Foliar gas exchange parameters were tightly linked to EAB induced canopy deterioration. Specifically,  $A_{\text{sat}}$  declined progressively from a maximum of  $14.5 \mu\text{mol m}^{-2} \text{s}^{-1}$  ( $\pm 0.39$ ) to  $6.69$  ( $\pm 0.35$ ) as ash trees became increasingly impacted by EAB (Figure 6A). Additionally, internal  $\text{CO}_2$  concentrations ( $C_i$ ) increased in leaves of ash canopies experiencing significant EAB damage (Figure 6B).

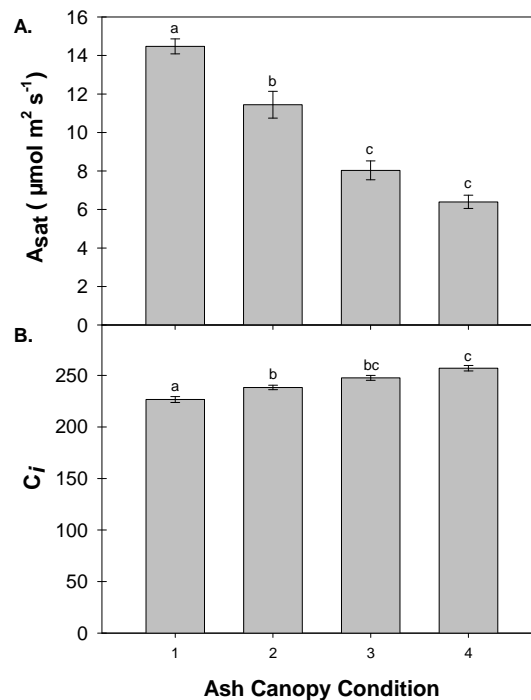


**Figure 6.** Mean light saturated photosynthetic rate ( $A_{\text{sat}}$ ; at 1600 PAR; panel (A)) and internal leaf  $\text{CO}_2$  concentration ( $C_i$ ; panel (B)) across foliage from ash trees of different ash condition classes. Letters represent significance levels determined by Tukey's HSD pairwise comparisons ( $p < 0.05$ ), error bars denote  $\pm 1$  SE.

## 4. Discussion

The results presented herein indicate that EAB larvae damage ash tree cambial tissue resulting in drastic changes to plant water relations leading to chronic water stress. As EAB symptom progression increased, SFD was reduced, inhibiting  $A_{\text{sat}}$  and reducing leaf size and mass. Increasing EAB larval feeding gallery cover or emergence holes within the stem have previously been linked to shifts in leaf and canopy level traits [24,32,35]. Although the experiment presented herein was not designed to investigate progressive canopy thinning as a mechanism by which ash trees can re-assimilate nutrients for later use as a means to cope with stress [45], our results lend support to this notion. Specifically, EAB damage resulted in significant reductions in leaf morphological characteristics (SA and DM; Figure 4a,b), consistent with leaf responses to water stress, yet SLA was conserved (Figure S1). The reductions in SA and dry mass seen in this study were comparable to those of Possen et al. [63]. However, the lack of a SLA response as EAB impacted trees contrasts the findings of Possen et al. [63] who observed a 5–10% increase in the SLA of *Betula* and *Populus* associated with wet and dry treatments. The  $\delta^{13}\text{C}$  isotopic enrichment of leaf tissue as ash trees progressed from healthy (AC 1) to heavily EAB impacted (AC 4) further supports the notion of EAB-induced chronic water stress in ash trees of this forest (Figure 5A) and is consistent with the previous reports of shifts in foliar carbon isotopic composition with differences in plant water use efficiency [64,65].

At the tree-level, sap flux rates were impacted by both biotic (EAB larvae) and abiotic (solar radiation and VPD) drivers (Table 2, Figure 1). The diurnal patterns of SFD of healthy trees reported

within this study are consistent with those of other deciduous species and are indicative of being driven by mostly abiotic factors [1,11,66–68]. Specifically, diel patterns of SFD are positively correlated with incoming solar radiation, as observed by Bovard et al. [1]. In our experiments EAB infestation altered the magnitude of the response to solar radiation as this response was larger on lightly EAB infested trees relative to moderately/heavily EAB infested ash trees (Figure 2). This result indicates the interaction of biotic factors with abiotic factors affecting ecosystem level fluxes of forest stands. Additionally, SFD was more positively related to VPD in non-infested or lightly EAB impacted trees relative to moderately and heavily EAB infested trees (Table 2, Figure 3).

Results suggest that EAB larvae cause significant damage to the cambial tissue of infested ash trees reducing not only the expected mass flow of nutrients between roots and shoots, but also the water flux. Larval damage reduced SFD in moderately and heavily EAB impacted trees relative to healthier trees (Table 2; Figure 3). These measurements reveal that moderately and heavily EAB impacted trees did not exhibit a compensatory increase in SFD to counter EAB activity, i.e., heavily impacted trees did not exhibit increased SFD in functioning xylem tissue to maintain canopy water relations. The consequence of xylem damage by EAB is the overall reduced water use. Reduced SFD in heavily EAB impacted trees paralleled reduced  $TWU_D$ , whereby lightly EAB impacted trees used 8 times more water per day compared to heavily EAB impacted trees (Figure 3). Daily water use of healthy ash trees observed in this study ( $13.4 \text{ kg day}^{-1}$ ) were lower than previously described for *F. excelsior* ( $27 \text{ kg day}^{-1}$ ), although focal trees in this study were nearly half the diameter and contained reduced sapwood area perhaps explaining this discrepancy [9]. We measured reduction of sap flux below the expected 1:1 relationship between relative daily sap flux and relative canopy cover as well as relative daily sap flux (a proxy for cambial damage [35]; see Figure S2). This relationship indicates that reductions in daily water use are not proportional to reductions in leaf area and therefore, the proportion of functional cambial tissue which governs mass flow is not solely responsible for the reductions seen in daily sap flux. Reductions in daily sap flux occur before canopy decline becomes apparent; indicating active down-regulation of photosynthesis or stomatal closure associated with EAB induced water stress (enriched foliar  $\delta^{13}\text{C}$  further supports the notion of direct EAB induced stomatal closure) and/or direct xylem tissue damage. Increased tree-level water stress has previously been linked to increased EAB larval numbers and mean larval mass [69], these results highlight how rapid alterations to plant water status may facilitate forest pest invasions.

The relationship between source activity and sink metabolism has been thoroughly demonstrated, and changes in sink demand (because of the likely EAB altered phloem transport) may be met with reduced photosynthetic rates and/or the accumulation of photosynthate (TNC) at the source tissues [70–72]. The lack of foliar TNC accumulation in heavily impacted trees relative to lightly infested trees does not support the occurrence of sink limitation (Table 3). The lack of a shift in foliar TNC associated with EAB is not consistent with girdling studies which indicate a regulation of photosynthesis by end-product accumulation [73–75]. The lack of end-product accumulation demonstrated here paired with the reduced leaf SA, enriched foliar  $\delta^{13}\text{C}$ , and reduced sap flux indicates broad damage to the vascular tissue caused by EAB larvae.

Other studies investigating different pests or diseases have found similar results. In a study of lodgepole pine inoculated with the blue stain fungi (*O. clavigerum*; associated with the mountain pine beetle, a common forest pest in the western US) it was observed that inoculated trees exhibited significantly reduced sap flow relative to control trees [76]. Similarly, Kirisits and Offenthaler [15] witnessed reductions in sap flow of Norway spruce (*Picea abies* (L.) H. Karst) following inoculation with *Ceratocystis polonica* (a fungal associate of the spruce bark beetle, *Ips typographus* L.). Additionally, Hultine et al. [18] observed reduced sap flux in tamarisk (*Tamarix* spp.) trees during a defoliation event by the saltcedar leaf beetle (*Diorhabda carinulata* Desbrochers). Results presented herein indicate that the EAB larval induced girdling of ash trees disrupts sapwood function, reducing water availability to leaves and altering the isotopic composition of leaf tissue (Table 1; Figure 5). Excavation of prepupal galleries that penetrate the xylem tissue may contribute to the EAB induced water stress [77].

The negative correlation observed between  $TWU_D$  and  $\delta^{13}C_{Leaf}$  indicates that the carbon isotopic composition of leaf tissue may be used as a proxy for whole plant water use ( $r_s = -0.9372$ ,  $p < 0.05$ ). The carbon isotopic signature of a leaf has been shown to be affected by the plants photosynthetic pathway, the diffusion of  $^{13}CO_2$  into the leaf, and the partial pressure of  $CO_2$  inside the leaf relative to the atmosphere [78]. In the current study, the shift in  $\delta^{13}C$  composition of leaf tissue resulted from high stomatal resistance in heavily infested trees (because of leaf level water stress), thus resulting in the reduced discrimination against the isotopically enriched  $^{13}C$  (and hence enriched  $^{13}C$  content in the photosynthetic tissue) (Table 1). While enriched foliar  $\delta^{13}C$  values of moderately and highly EAB impacted trees are consistent with several of our proposed mechanisms (stem girdling and foliar carbohydrate accumulation), when paired with the reduction in  $TWU_D$ , these results support the hypothesis that inhibited water and nutrient movement between roots and shoots associated with EAB infestation is due to the larval feeding which damages cambial tissue. Although the down regulation of photosynthesis by accumulation of carbohydrates will also result in photoinhibition, the absence of foliar TNC loading in ash trees with moderate to high levels of EAB-induced canopy decline suggests carbohydrate accumulation is not playing a significant role.

In temperate deciduous forests with a high leaf area index, transpiration can represent a substantial portion of the water budget, thus tree mortality can greatly impact forest hydrology [79]. We calculated  $TWU_D$  in healthy ash trees at  $\sim 13.5 \text{ kg day}^{-1}$  compared to  $\sim 2 \text{ kg day}^{-1}$  in heavily infested trees. Scaling those rates to a forest where ash represents  $\sim 80\%$  of the basal area, such a disturbance could result in a significant alteration of the hydrological cycle, and the energy balance of ecosystems with potential impacts to the regional climate system [37]. The reduced sap flux and  $TWU_D$  could either increase available soil moisture or reduce soil moisture content (via canopy thinning which could increase soil temperature and evaporation or from reduced hydraulic lift). While nocturnal hydraulic lift has been widely observed in arid systems, it remains uncertain how widespread the phenomenon of hydraulic lift is in deciduous forest systems [80–83].

As a result of resource limitations the number of replicates included in the study was limited, as such trees in categories AC 2 and AC 3 were pooled (despite the recognition that underlying stress levels may differ). As such, caution should be utilized when extrapolating these findings to trees exhibiting intermediate decline patterns. Furthermore, due to the fact that SFD rates of the ash trees in this study were not measured across the entire growing season and that SFD rates of non-ash species were not measured, the authors felt that it was inappropriate to scale EAB induced ash tree decline to annual forest ecosystem water use. However, ash represents an ecologically significant component of riparian forests across the eastern United States and its exclusion from the landscape may result in considerable change to the ecosystem functioning of these sensitive systems [6,28,57].

## 5. Conclusions

This study reveals the negative impacts tree boring insects on tree water use and highlights the canopy decline, leaf morphological and chemical shifts that accompany tree-level EAB infestation. Our results demonstrate that as ash trees succumb to increased levels of EAB stress, they exhibit reduced canopy cover (via ash canopy condition), reduced leaf area, and reduced leaf dry mass, but no shift in SLA or foliar NSC concentrations (Figure 4 and Figure S2, Table 3). Our results support the theory that the serpentine galleries created by EAB larval feeding results in tree-level water stress as indicated by significant reductions in SFD and subsequently  $TWU_D$  (Figures 1–3). Reductions in relative  $TWU_D$  were greater than would have been expected if  $TWU_D$  was directly proportional to relative canopy cover or the proportion of intact cambium, suggesting active down-regulation of photosynthesis (Figures S1 and S2). This theory is also consistent with the depleted (more negative) carbon isotopic composition of leaves from trees in AC 1 relative to AC 4 (Table 1; Figure 5A). The significant reduction in  $TWU_D$  caused by EAB, paired with the rapid decline of infested trees, highlights the potentially severe impacts of this non-native forest pest on individual trees and forest

ecosystems. Rapid alterations in the water table caused by reductions in tree water use could have consequences for successional dynamics.

**Supplementary Materials:** The following are available online at <http://www.mdpi.com/1999-4907/9/6/301/s1>, Figure S1: Relationship between leaf dry mass and surface area, Figure S2: Relationship between relative daily water use and relative canopy cover.

**Author Contributions:** C.E.F., D.J.L., and M.A.G.-M. conceived and designed the experiment; K.S.K. provided plot access; C.E.F. conducted the field work, sampling and analysis; C.E.F. and D.J.L. analyzed the data; C.E.F. and D.J.L. wrote the manuscript; M.A.G.-M. edited the manuscript.

**Acknowledgments:** This research was supported in part by the National Science Foundation Grant DGE-0549245 (C.E.F.), the University of Illinois at Chicago, and the United States Department of Agriculture Northern Research Station. Additionally, we thank J. Rucks for her assistance with labile carbohydrate analyses.

**Conflicts of Interest:** The authors declare no conflict of interest.

## References

1. Bovard, B.D.; Curtis, P.S.; Vogel, C.S.; Su, H.-B.; Schmid, H.P. Environmental controls on sap flow in a northern hardwood forest. *Tree Physiol.* **2005**, *25*, 31–38. [[CrossRef](#)] [[PubMed](#)]
2. Oren, R.; Phillips, N.; Ewers, B.E.; Pataki, D.E.; Megonigal, J.P. Sap-Flux-Scaled Transpiration Responses To Light, Vapor Pressure Deficit, and Leaf Area Reduction in a flooded *Taxodium distichum* forest. *Tree Physiol.* **1999**, *19*, 337–347. [[CrossRef](#)] [[PubMed](#)]
3. Lösch, R. Plant Water Relations. In *Progress in Botany: Genetics Cell Biology and Physiology Systematics and Comparative Morphology Ecology and Vegetation Science*; Esser, K., Kadereit, J.W., Lüttge, U., Runge, M., Eds.; Springer: Berlin/Heidelberg, Germany, 1999; pp. 193–233. ISBN 978-3-642-59940-8.
4. Wullschlegel, S.D.; Meinzer, F.C.; Vertessy, R.A. A Review of Whole-Plant Water Use Studies in Tree. *Tree Physiol.* **1998**, *18*, 499–512. [[CrossRef](#)] [[PubMed](#)]
5. Hubbard, R.M.; Rhoades, C.C.; Elder, K.; Negron, J. Changes in transpiration and foliage growth in lodgepole pine trees following mountain pine beetle attack and mechanical girdling. *For. Ecol. Manag.* **2013**, *289*, 312–317. [[CrossRef](#)]
6. Flower, C.E.; Gonzalez-Meler, M.A. Responses of temperate forest productivity to insect and pathogen disturbances. *Annu. Rev. Plant Biol.* **2015**, *66*, 547–569. [[CrossRef](#)] [[PubMed](#)]
7. Lagergren, F.; Lindroth, A. Transpiration response to soil moisture in pine and spruce trees in Sweden. *Agric. For. Meteorol.* **2002**, *112*, 67–85. [[CrossRef](#)]
8. Lu, P.; Urban, L.; Zhao, P. Granier's thermal dissipation probe (TDP) method for measuring Sap Flow in trees: theory and practice. *Acta Bot. Sin.* **2004**, *46*, 631–646.
9. Hölscher, D.; Koch, O.; Korn, S.; Leuschner, C. Sap flux of five co-occurring tree species in a temperate broad-leaved forest during seasonal soil drought. *Trees* **2005**, *19*, 628–637. [[CrossRef](#)]
10. Gebauer, T.; Horna, V.; Leuschner, C. Variability in radial sap flux density patterns and sapwood area among seven co-occurring temperate broad-leaved tree species. *Tree Physiol.* **2008**, *28*, 1821–1830. [[CrossRef](#)] [[PubMed](#)]
11. Oren, R.; Pataki, D.E. Transpiration in response to variation in microclimate and soil moisture in southeastern deciduous forests. *Oecologia* **2001**, *127*, 549–559. [[CrossRef](#)] [[PubMed](#)]
12. Granier, A. Evaluation of transpiration in a Douglas-fir stand by means of sap flow measurements. *Tree Physiol.* **1987**, *3*, 309–320. [[CrossRef](#)] [[PubMed](#)]
13. Ploetz, R.C.; Schaffer, B.; Vargas, A.I.; Konkol, J.L.; Salvatierra, J.; Wideman, R. Impact of Laurel Wilt, Caused by *Raffaelea lauricola*, on Leaf Gas Exchange and Xylem Sap Flow in Avocado, *Persea americana*. *Phytopathology* **2015**, *105*, 433–440. [[CrossRef](#)] [[PubMed](#)]
14. Urban, J.; Dvořák, M. Sap flow-based quantitative indication of progression of Dutch elm disease after inoculation with *Ophiostoma novo-ulmi*. *Trees Struct. Funct.* **2014**, *28*, 1599–1605. [[CrossRef](#)]
15. Kirisits, T.; Offenthaler, I. Xylem sap flow of Norway spruce after inoculation with the blue-stain fungus *Ceratocystis polonica*. *Plant Pathol.* **2002**, *51*, 359–364. [[CrossRef](#)]
16. Park, J.-H.; Juzwik, J.; Cavender-Bares, J. Multiple *Ceratocystis smalleyi* infections associated with reduced stem water transport in bitternut hickory. *Phytopathology* **2013**, *103*, 565–574. [[CrossRef](#)] [[PubMed](#)]



17. Schäfer, K.V.R.; Clark, K.L.; Skowronski, N.; Hamerlynck, E.P. Impact of insect defoliation on forest carbon balance as assessed with a canopy assimilation model. *Glob. Chang. Biol.* **2010**, *16*, 546–560. [[CrossRef](#)]
18. Hultine, K.R.; Nagler, P.L.; Morino, K.; Bush, S.E.; Burtch, K.G.; Dennison, P.E.; Glenn, E.P.; Ehleringer, J.R. Sap flux-scaled transpiration by tamarisk (*Tamarix* spp.) before, during and after episodic defoliation by the saltcedar leaf beetle (*Diorhabda carinulata*). *Agric. For. Meteorol.* **2010**, *150*, 1467–1475. [[CrossRef](#)]
19. Bauer, L.; Haack, R.A.; Miller, D.; Petrice, T.; Liu, H. Emerald ash borer life cycle. In Proceedings of the Emerald Ash Borer Research and Technology Development Meeting, Port Huron, MI, USA, 30 September–1 October 2003; FHTET-2004-02. USDA Forest Service, Forest Health Technology Enterprise Team: Morgantown, WV, USA, 2004; p. 8.
20. Siegert, N.W.; McCullough, D.G.; Liebhold, A.M.; Telewski, F.W. Dendrochronological reconstruction of the epicentre and early spread of emerald ash borer in North America. *Divers. Distrib.* **2014**, *20*, 847–858. [[CrossRef](#)]
21. Wang, X.; Yang, Z.; Gould, J.; Zhang, Y.; Liu, G.; Liu, E. The biology and ecology of the emerald ash borer, *Agrilus planipennis*, in China. *J. Insect Sci.* **2010**, *10*, 128. [[CrossRef](#)] [[PubMed](#)]
22. Cappaert, D.; McCullough, D.G.; Poland, T.M.; Siegert, N.W. Emerald ash borer in north america a research and regulatory challenge. *Am. Entomol.* **2005**, *51*, 152–165. [[CrossRef](#)]
23. Herms, D.A.; McCullough, D.G. Emerald Ash Borer Invasion of North America: History, Biology, Ecology, Impacts, and Management. *Annu. Rev. Entomol.* **2014**, *59*, 13–30. [[CrossRef](#)] [[PubMed](#)]
24. Rebek, E.J.; Herms, D.A.; Smitley, D.R. Interspecific variation in resistance to emerald ash borer (Coleoptera: Buprestidae) among North American and Asian ash (*Fraxinus* spp.). *Environ. Entomol.* **2008**, *37*, 242–246. [[CrossRef](#)]
25. Anulewicz, A.C.; McCullough, D.G.; Cappaert, D.L.; Poland, T.M. Host range of the emerald ash borer (*Agrilus planipennis* Fairmaire) (Coleoptera: Buprestidae) in North America: results of multiple-choice field experiments. *Environ. Entomol.* **2008**, *37*, 230–241. [[CrossRef](#)]
26. Cipollini, D. White fringetree as a novel larval host for emerald ash borer. *J. Econ. Entomol.* **2015**, *108*, 370–375. [[CrossRef](#)] [[PubMed](#)]
27. Pugh, S.A.; Liebhold, A.M.; Morin, R.S. Changes in ash tree demography associated with emerald ash borer invasion, indicated by regional forest inventory data from the Great Lakes States. *Can. J. For. Res.* **2011**, *41*, 2165–2175. [[CrossRef](#)]
28. Flower, C.E.; Knight, K.S.; Gonzalez-Meler, M.A. Impacts of the emerald ash borer (*Agrilus planipennis* Fairmaire) induced ash (*Fraxinus* spp.) mortality on forest carbon cycling and successional dynamics in the eastern United States. *Biol. Invasions* **2013**, *15*, 931–944. [[CrossRef](#)]
29. MacFarlane, D.W.; Meyer, S.P. Characteristics and distribution of potential ash tree hosts for emerald ash borer. *For. Ecol. Manag.* **2005**, *213*, 15–24. [[CrossRef](#)]
30. Burns, R.; Honkala, B. *Silvics of North America, Vol. 2: Hardwoods. Agriculture Handbook 654*; United States Department of Agriculture Forest Service: Washington, DC, USA, 1990.
31. McCullough, D.G.; Poland, T.M.; Cappaert, D. Attraction of the emerald ash borer to ash trees stressed by girdling, herbicide treatment, or wounding. *Can. J. For. Res.* **2009**, *39*, 1331–1345. [[CrossRef](#)]
32. Smitley, D.; Davis, T.; Rebek, E. Progression of ash canopy thinning and dieback outward from the initial infestation of emerald ash borer (Coleoptera: Buprestidae) in southeastern Michigan. *J. Econ. Entomol.* **2008**, *101*, 1643–1650. [[CrossRef](#)] [[PubMed](#)]
33. Knight, K.S.; Brown, J.P.; Long, R.P. Factors affecting the survival of ash trees (*Fraxinus* spp.) infested by emerald ash borer (*Agrilus planipennis*). *Biol. Invasions* **2013**, *15*, 371–383. [[CrossRef](#)]
34. Flower, C.E.; Lynch, D.J.; Knight, K.S.; González-Meler, M.A. EAB induced tree mortality impacts tree water use and ecosystem respiration in an experimental forest. In Proceedings of the Emerald Ash Borer National Research and Technology Development Meeting, Wooster, OH, USA, 12–13 October 2011; FHTET-2011-06. pp. 115–116.
35. Flower, C.E.; Knight, K.S.; Rebbeck, J.; Gonzalez-Meler, M.A. The relationship between the emerald ash borer (*Agrilus planipennis*) and ash (*Fraxinus* spp.) tree decline: Using visual canopy condition assessments and leaf isotope measurements to assess pest damage. *For. Ecol. Manag.* **2013**, *303*, 143–147. [[CrossRef](#)]
36. Telander, A.C.; Slesak, R.A.; D’Amato, A.W.; Palik, B.J.; Brooks, K.N.; Lenhart, C.F. Sap flow of black ash in wetland forests of northern Minnesota, USA: Hydrologic implications of tree mortality due to emerald ash borer. *Agric. For. Meteorol.* **2015**, *206*, 4–11. [[CrossRef](#)]



37. Drewniak, B.; Gonzalez-Meler, M.A. Earth system model needs for including the interactive representation of nitrogen deposition and drought effects on forested ecosystems. *Forests* **2017**, *8*, 267. [[CrossRef](#)]
38. Paul, M.J.; Pellny, T.K. Carbon metabolite feedback regulation of leaf photosynthesis and development. *J. Exp. Bot.* **2003**, *54*, 539–547. [[CrossRef](#)] [[PubMed](#)]
39. Rashke, K. Stomatal action. *Annu. Rev. Plant Physiol.* **1975**, *26*, 309–340. [[CrossRef](#)]
40. Collatz, G.J.; Ball, J.T.; Grivet, C.; Berry, J.A. Physiological and environmental regulation of stomatal conductance, photosynthesis and transpiration—A model that includes a laminar boundary-layer. *Agric. For. Meteorol.* **1991**, *54*, 107–136. [[CrossRef](#)]
41. Sperry, J.S. Hydraulic constraints on plant gas exchange. *Agric. For. Meteorol.* **2000**, *104*, 13–23. [[CrossRef](#)]
42. Setter, T.L.; Brun, W.A.; Brenner, M.L. Effect of obstructed translocation on leaf abscisic Acid, and associated stomatal closure and photosynthesis decline. *Plant Physiol.* **1980**, *65*, 1111–1115. [[CrossRef](#)] [[PubMed](#)]
43. Cheng, J.; Fan, P.; Liang, Z.; Wang, Y.; Niu, N.; Li, W.; Li, S. Accumulation of End Products in Source Leaves Affects Photosynthetic Rate in Peach via Alteration of Stomatal Conductance and Photosynthetic Efficiency. *J. Am. Soc. Hortic. Sci.* **2009**, *134*, 667–676.
44. Azcón-Bieto, J.; Osmond, C.B. Relationship between photosynthesis and respiration—The effect of carbohydrate status on the rate of CO<sub>2</sub> production by respiration in darkened and illuminated wheat leaves. *Plant Physiol.* **1983**, *71*, 574–581. [[CrossRef](#)] [[PubMed](#)]
45. Munné-Bosch, S.; Alegre, L. Die and let live: Leaf senescence contributes to plant survival under drought stress. *Funct. Plant Biol.* **2004**, *31*, 203–216. [[CrossRef](#)]
46. Otieno, D.O.; Schmidt, M.W.T.; Adiku, S.; Tenhunen, J. Physiological and morphological responses to water stress in two Acacia species from contrasting habitats. *Tree Physiol.* **2005**, *25*, 361–371. [[CrossRef](#)] [[PubMed](#)]
47. Slesak, R.A.; Lenhart, C.F.; Brooks, K.N.; D’Amato, A.W.; Palik, B.J. Water table response to harvesting and simulated emerald ash borer mortality in black ash wetlands in Minnesota, USA. *Can. J. For. Res.* **2014**, *44*, 961–968. [[CrossRef](#)]
48. Saurer, M.; Siegwolf, R.T.W.; Schweingruber, F.H. Carbon isotope discrimination indicates improving water-use efficiency of trees in northern Eurasia over the last 100 years. *Glob. Chang. Biol.* **2004**, *10*, 2109–2120. [[CrossRef](#)]
49. Flower, C.E.; Dalton, J.E.; Knight, K.S.; Brikha, M.; Gonzalez-Meler, M.A. To treat or not to treat: Diminishing effectiveness of emamectin benzoate tree injections in ash trees heavily infested by emerald ash borer. *Urban For. Urban Green.* **2015**, *14*. [[CrossRef](#)]
50. Ford, C.R.; McGuire, M.A.; Mitchell, R.; Teskey, R.O. Assessing variations in the radial profile of sap flow density in *Pinus* species and its effects on daily water use. *Tree Physiol.* **2004**, *24*, 241–249. [[CrossRef](#)] [[PubMed](#)]
51. Kelliher, F.M.; Kostner, B.M.M.; Hollinger, D.Y.; Byers, J.N.; Hunt, J.E.; McSeveny, T.M.; Meserth, R.; Weir, P.L.; Schulze, E.D. Evaporation, Xylem Sap Flow, and Tree Transpiration in a New-Zealand Broad-Leaved Forest. *Agric. For. Meteorol.* **1992**, *62*, 53–73. [[CrossRef](#)]
52. Young, A.; Mitchell, N. Microclimate and vegetation edge effects in a fragmented podocarp-broadleaf forest in New Zealand. *Biol. Conserv.* **1994**, *67*, 63–72. [[CrossRef](#)]
53. Veen, A.W.L.; Klaassen, W.; Kruijt, B.; Hutjes, R.W.A. Forest edges and the soil-vegetation-atmosphere interaction at the landscape scale: The state of affairs. *Prog. Phys. Geogr.* **1996**, *20*, 292–310. [[CrossRef](#)]
54. Davies-Colley, R.J.; Payne, G.W.; Van Elswijk, M. Microclimate gradients across a forest edge. *N. Z. J. Ecol.* **2000**, *24*, 111–121.
55. Herbst, M.; Roberts, J.M.; Rosier, P.T.W.; Taylor, M.E.; Gowing, D.J. Edge effects and forest water use: A field study in a mixed deciduous woodland. *For. Ecol. Manag.* **2007**, *250*, 176–186. [[CrossRef](#)]
56. Flower, C.E.; Knight, K.S.; González-Meler, M.A. Using stable isotopes as a tool to investigate the impacts of EAB on tree physiology and EAB spread. In Proceedings of the Emerald Ash Borer Research and Technology Development Meeting, Pittsburgh, PA, USA, 20–21 October 2009; FHTET-2010-01. USDA Forest Service, Forest Health Technology Enterprise Team: Morgantown, WV, USA, 2010; pp. 54–55.
57. Smith, A. Effects of Community Structure on Forest Susceptibility and Response to the Emerald Ash Borer iNvasion of the Huron River Watershed in Southeast Michigan. Master’s Thesis, The Ohio State University, Columbus, OH, USA, 2006.
58. Granier, A. A new method of sap flow measurement in tree stems. *Ann. Des. Sci. For.* **1985**, *42*, 193–200. [[CrossRef](#)]

59. Do, F.; Rocheteau, A. Influence of natural temperature gradients on measurements of xylem sap flow with thermal dissipation probes. 2. Advantages and calibration of a noncontinuous heating system. *Tree Physiol.* **2002**, *22*, 649–654. [[CrossRef](#)] [[PubMed](#)]
60. Meadows, J.S.; Hodges, J.D. Sapwood area as an estimator of leaf area and oliar weight in cherrybark oak and green ash. *For. Sci.* **2001**, *48*, 69–76.
61. Jones, M.G.; Outlaw, W.H.; Lowry, O.H. Enzymic assay of  $10^{-7}$  to  $10^{-14}$  moles of sucrose in plant tissues. *Plant Physiol.* **1977**, *60*, 379–383. [[CrossRef](#)] [[PubMed](#)]
62. Curtis, P.S.; Vogel, C.S.; Wang, X.Z.; Pregitzer, K.S.; Zak, D.R.; Lussenhop, J.; Kubiske, M.; Teeri, J.A. Gas exchange, leaf nitrogen, and growth efficiency of *Populus tremuloides* in a CO<sub>2</sub>-enriched atmosphere. *Ecol. Appl.* **2000**, *10*, 3–17.
63. Possen, B.J.H.M.; Oksanen, E.; Rousi, M.; Ruhanen, H.; Ahonen, V.; Tervahauta, A.; Heinonen, J.; Heiskanen, J.; Kärenlampi, S.; Vapaavuori, E. Adaptability of birch (*Betula pendula* Roth) and aspen (*Populus tremula* L.) genotypes to different soil moisture conditions. *For. Ecol. Manag.* **2011**, *262*, 1387–1399. [[CrossRef](#)]
64. Farquhar, G.D.; Ball, M.C.; Roksandic, Z.; City, C. Effect of salinity and humidity on  $\delta^{13}C$  value of halophytes-evidence for diffusional isotope fractionation determined by the ratio of intercellular/atmospheric partial pressure of CO<sub>2</sub> under different environmental conditions. *Oecologia* **1982**, *52*, 121–124. [[CrossRef](#)] [[PubMed](#)]
65. Farquhar, G.D.; Richards, R.A. Isotopic composition of plant carbon correlates with water-use efficiency of wheat genotypes. *Aust. J. Plant Physiol.* **1984**, *11*, 539–552. [[CrossRef](#)]
66. Granier, A.; Anfodillo, T.; Sabatti, M.; Cochard, H.; Dreyer, E.; Tomasi, M.; Valentini, R.; Bréda, N. Axial and radial water flow in the trunk of oak trees: a quantitative and qualitative analysis. *Tree Physiol.* **1994**, *14*, 1383–1396. [[CrossRef](#)] [[PubMed](#)]
67. Lu, P.; Biron, P.; Breda, N.; Granier, A. Water relations of adult Norway spruce (*Picea abies* (L) Karst) under soil drought in the Vosges mountains: water potential, stomatal conductance and transpiration. *Ann. For. Sci.* **1995**, *52*, 117–129. [[CrossRef](#)]
68. Stöhr, A.; Lösch, R. Xylem sap flow and drought stress of *Fraxinus excelsior* saplings. *Tree Physiol.* **2004**, *24*, 169–180. [[CrossRef](#)] [[PubMed](#)]
69. Chakraborty, S.; Whitehill, J.G.A.; Hill, A.L.; Opiyo, S.O.; Cipollini, D.; Herms, D.A.; Bonello, P. Effects of water availability on emerald ash borer larval performance and phloem phenolics of Manchurian and black ash. *Plant Cell Environ.* **2014**, *37*, 1009–1021. [[CrossRef](#)] [[PubMed](#)]
70. Azcón-Bieto, J. Inhibition of photosynthesis by carbohydrates in wheat leaves. *Plant Physiol.* **1983**, *73*, 681–686. [[CrossRef](#)] [[PubMed](#)]
71. Paul, M.J.; Foyer, C.H. Sink regulation of photosynthesis. *J. Exp. Bot.* **2001**, *52*, 1383–1400. [[CrossRef](#)] [[PubMed](#)]
72. Iglesias, D.J.; Lliso, I.; Tandeo, F.R.; Talon, M. Regulation of photosynthesis through source: sink imbalance in citrus mediated by carbohydrate content in leaves. *Physiol. Plant.* **2002**, *116*, 563–572. [[CrossRef](#)]
73. Goldschmidt, E.E.; Huber, S.C. Regulation of photosynthesis by end-product accumulation in leaves of plants storing starch, sucrose, and hexose sugars. *Plant Physiol.* **1992**, *99*, 1443–1448. [[CrossRef](#)] [[PubMed](#)]
74. Jordan, M.-O.; Habib, R. Mobilizable carbon reserves in young peach trees as evidenced by trunk girdling experiments. *J. Exp. Bot.* **1996**, *47*, 79–87. [[CrossRef](#)]
75. Myers, D.; Thomas, R.; DeLucia, E. Photosynthetic responses of loblolly pine (*Pinus taeda*) needles to experimental reduction in sink demand. *Tree Physiol.* **1999**, *19*, 235–242. [[CrossRef](#)] [[PubMed](#)]
76. Yamaoka, Y.; Swanson, R.; Hiratsuka, Y. Inoculation of lodgepole pine with four blue-stain fungi associated with mountain pine beetle, monitored by a heat pulse velocity (HPV) instrument. *Can. J. For. Res.* **1990**, *20*, 31–36. [[CrossRef](#)]
77. Mack, R. Characterization of emerald ash borer (EAB) pupal chamber location in ash log sections. In *2014 Emerald Ash Borer National Research and Technology Development Meeting*; Buck, J., Parra, G., Lance, D., Reardon, R., Binion, D., Eds.; USDA Forest Service, Forest Health Technology Enterprise Team: Morgantown, WV, USA, 2015; p. 52.
78. Farquhar, G.D.; O’Leary, M.H.; Berry, J.A. On the relationship between carbon isotope discrimination and the intercellular carbon dioxide concentration in leaves. *Aust. J. Plant Physiol.* **1982**, *9*, 121–137. [[CrossRef](#)]

79. Running, S.W.; Coughlan, J.C. A general-model of forest ecosystem processes for regional applications. I. Hydrologic balance, canopy gas-exchange and primary production processes. *Ecol. Model.* **1988**, *42*, 125–154. [[CrossRef](#)]
80. Richards, J.; Caldwell, M. Hydraulic lift: Substantial nocturnal water transport between soil layers by *Artemisia tridentata* roots. *Oecologia* **1987**, *73*, 486–489. [[CrossRef](#)] [[PubMed](#)]
81. Caldwell, M.M.; Richards, J.H. Hydraulic lift: water efflux from upper roots improves effectiveness of water uptake by deep roots. *Oecologia* **1989**, *79*, 1–5. [[CrossRef](#)] [[PubMed](#)]
82. Dawson, T.E. Determining water use by trees and forests from isotopic, energy balance and transpiration analyses: the roles of tree size and hydraulic lift. *Tree Physiol.* **1996**, *16*, 263–272. [[CrossRef](#)] [[PubMed](#)]
83. Dawson, T.E. Hydraulic lift and water use by plants: implications for water balance, performance and plant-plant interactions. *Oecologia* **1993**, *95*, 565–574. [[CrossRef](#)] [[PubMed](#)]



© 2018 by the authors. Licensee MDPI, Basel, Switzerland. This article is an open access article distributed under the terms and conditions of the Creative Commons Attribution (CC BY) license (<http://creativecommons.org/licenses/by/4.0/>).